Exp. Anim. 67(3), 383–392, 2018

—Original—

A rat model for pituitary stalk electric lesion-induced central diabetes insipidus: application of 3D printing and further outcome assessments

Zhanpeng FENG[1)], Yichao OU[1)], Mingfeng ZHOU[1)], Guangsen WU[2)], Linzi MA[2)], Yun BAO[1)], Binghui QIU[1)], and Songtao QI[1)]

[1)]*Department of Neurosurgery, Nanfang Hospital, Southern Medical University, No. 1838, North of Guangzhou Avenue, No. 1038, North Guangzhou Avenue, Baiyun District, Guangzhou 510515, P.R. China*
[2)]*The First School of Clinical Medicine, Southern Medical University, No. 1023, South Shatai Road, Baiyun District, Guangzhou 510515, P.R. China*

Abstract: A stable and reproducible rat injury model is not currently available to study central diabetes insipidus (CDI) and the neurohypophyseal system. In addition, a system is needed to assess the severity of CDI and measure the accompanying neurobiological alterations. In the present study, a 3D-printed lesion knife with a curved head was designed to fit into the stereotaxic instrument. The neuro-anatomical features of the brain injury were determined by *in vivo* magnetic resonance imaging (MRI) and arginine vasopressin (AVP) immunostaining on brain sections. Rats that underwent pituitary stalk electrical lesion (PEL) exhibited a tri-phasic pattern of CDI. MRI revealed that the hyperintenseT1-weighted signal of the pituitary stalk was interrupted, and the brain sections showed an enlarged end proximal to the injury site after PEL. In addition, the number of AVP-positive cells in supraoptic nucleus (SON) and paraventricular nucleus (PVN) decreased after PEL, which confirmed the success of the CDI model. Unlike hand-made tools, the 3D-printed lesion knives were stable and reproducible. Next, we used an ordinal clustering method for staging and the k-means' clustering method to construct a CDI index to evaluate the severity and recovery of CDI that could be used in other multiple animals, even in clinical research. In conclusion, we established a standard PEL model with a 3D-printed knife tool and proposed a CDI index that will greatly facilitate further research on CDI.
Key words: 3D printing, central diabetes insipidus, magnetic resonance imaging, pituitary stalk injury, rats model

Introduction

Water and electrolyte imbalances are common after any injury to the hypothalamo-neurohypophyseal system (HNS) [5, 8, 9, 11, 17, 25], in which the pituitary stalk can be easily damaged and result in a severe hypothalamic dysfunction.

The role of magnocellular arginine vasopressin (AVP) and oxytocin (OXT) in the hypothalamic–pituitary axis, which includes the supraoptic nucleus (SON) and paraventricular nucleus (PVN), is related to the regulation of fluid balance. Furthermore, the axons of these neurons project into the posterior pituitary through a part of the median eminence (ME) [21]. In the HNS, there are two

(Received 23 January 2018 / Accepted 28 March 2018 / Published online in J-STAGE 20 April 2018)
Addresses corresponding: S. Qi, Department of Neurosurgery, Nanfang Hospital, Southern Medical University, No. 1838, North of Guangzhou Avenue, No. 1038, North Guangzhou Avenue, Baiyun District, Guangzhou 510515, P.R. China

main ways to damage this area to model CDI: targeted injury in the pituitary stalk through the subtemporal [1–4] or a parietal approach [6, 8, 11, 13, 19] and hypophysectomy through the peripharyngeal [25, 26, 28, 29] or transauricular approach [12, 22, 23].

Compared with hypophysectomy, targeted injury to the pituitary stalk requires that the adenohypophysis remain undamaged [13, 19]. Since manual tools are fraught with differences in skill and precision, building a stable and reproducible pituitary stalk lesion model in rats and making suitable assessments regarding CDI are needed.

Materials and Methods

Animals

Male Sprague–Dawley rats with an average body weight of 200 g (180–220 g) were used in the present experiments. The animals were housed in independent metabolic cages, in a temperature-controlled room with daily light and dark cycle. Food and water was provided without restrictions, both before and after surgery. All procedures were in accordance with our institutional guidelines and were approved by the regional ethics committee.

Designing a lesion knife by 3D printing

Knives were designed using AutoCAD 2014 software (Autodesk software) to fit into the stereotaxic instrument (51600, Stoelting) used in our experiments. A wedge was incorporated at the tail of the knives to match the probe holder, as the corner clamp of the instrument (Fig. 1). The head of the knives were 2.5-mm wide by 1-mm thick, with a radius that could fit the base skull of rats (Fig. 1C). The design files were exported from the inventor in the STEP format and printed by SLM printer (SLM Solutions) at a local professional company. Although aluminum alloy 7075 was used to fabricate the knives used in this study, the 3-D printed knives were coated with insulation oil till 0.2 mm from the head.

Pituitary stalk electric lesion (PEL) and experimental protocol

The animals were housed in independent metabolic cages for 3 days before surgery and their water intake and urine output were monitored daily. PEL was performed by parietal approach. The animals were first anesthetized with 5% isoflurane with the help of a rat gas mask fitted into the platform of the stereotaxic instrument. The rats were anesthetized for 2 min, during which isoflurane was maintained at 1.5–2% in air flowing at 0.5 l/min inside the closed chamber. The rats were then mounted on a stereotaxic frame with nose down 3.3 mm and the skull was opened by removing a 3 by 3 mm square (approx.) of bone (Fig. 1). The knife was lowered into the coronal plane 3.8-mm caudal to bregma in the sagittal midline until it reached the floor of the skull base which is over 8 mm beneath the surface of the brain. To trigger PEL, a cathodic current of 500 μA was applied for 40 s with a constant power supply output (53500, UGO Basile). For sham surgery, the knife was lowered 8 mm beneath the surface of the brain and no electric current was applied to avoid an injury on the pituitary stalk. After surgery, the animals were put back to metabolic cages and their water intake, urine output and specific gravity of urine were monitored daily for 28 days post-operation.

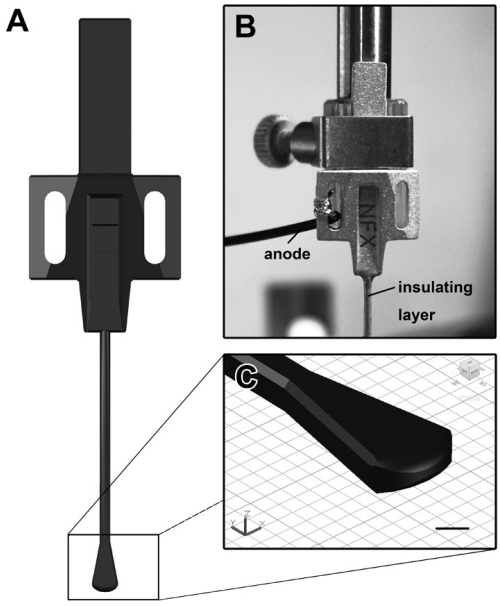

Fig. 1. A knife with a curved head that was applied to the lesion in the pituitary stalk of rats. A: The layout of the lesion knife; B: The knife was assembled with the probe holder, corner clamp and the anode; C: A magnified view of the head of the knife from A (black box). Scale bar=1 mm.

Measurement of serum AVP

The serum AVP levels were quantified using an ELISA kit (74-VSPHU-E01.1, ALPCO). At day 28 after operation, blood samples were collected from the retro-orbit-

al sinus. After centrifugation, the supernatant serum was collected then AVP levels were detected according to the manufacturer's method.

In vivo MRI

Scans was performed on a 7.0 T Bruker Pharmascan (Bruker Biospin) equipped with a 6-cm volume resonator using Paravision 5.0. The rats were anaesthetized with isoflurane during the MRI scans. A Gd-DTPA enhanced T1-weight and T2-weight with the following parameters was used: TR=1,500 ms, TE=11.2 ms; TR=2,500 ms, TE=35 ms, slice thickness=0.5 mm. T1-weight scans were captured immediately after 200 μl Gd-DTPA was administered by intraperitoneal injection.

Perfusion and tissue processing for immunohistochemistry

At the end of the postoperative survival period, the rats were deeply anesthetized with sodium pentobarbital (80 mg/kg), then were perfused intracardially with normal saline, followed by cool 4% paraformaldehyde in 0.1 M phosphate buffer saline (PBS) (pH 7.4). For sagittal brain paraffin slices, sheeting base skull was reserved and thinned by electric drill. Then brain along with bone was placed in 4% formaldehyde for at least 24 h, followed by gradient ethanol dehydration and infiltration of histological samples in tissue processor, embedded in paraffin, and 4 μm thin-sectioned. For coronal cryostat brain sectioning, the brains were normally removed from the skull and placed in 4% formaldehyde for at least 24 h. After post-fixation, the brain was placed in 15% and 30% sucrose at 4°C, respectively, then was embedded in O.C.T. Compound. Coronal sections were cut at 40 μm on a freezing microtome. Sections were collected and rinsed in 0.1 M phosphate buffered saline (PBS, pH 7.4).

Immunocytochemistry

For immunohistochemical staining, sagittal paraffin tissue sections were stained using the peroxidase-labeled antibody method. The tissue sections were deparaffinized with xylene, and rinsed with 100% ethanol. After endogenous peroxidase was blocked with 0.3% H_2O_2 at room temperature for 30 min and antigen retrieval with high pressure and temperature, the sections were rinsed with 0.01 M phosphate buffered saline (PBS), then blocked with goat serum for 1h at room temperature. A rabbit polyclonal antibody against AVP (1:1,000, Millipore) was placed on the tissue sections, and incubated at 4°C overnight in humidified box. After the sections were rinsed with PBS, anti-rabbit antibody (1:500, abclonal) was added to the sections as the secondary antibody, and incubated at room temperature for 30 min. The sections were then rinsed with PBS, and the anti-gen-antibody complexes were rendered visible by reaction with 50 mM Tris-HCl buffer (pH7.6) containing 0.05% 3,3′-diaminobenzidine-4HCl (DAB). The sections were also stained with hematoxylin for 2 min for nuclear staining. For coronal cryostat brain sections staining, sections were rinsed with PBS, and blocked with non-specific antigen goat serum for 1h at room temperature. The sections were incubated overnight at 4°C with a rabbit polyclonal antibody against AVP (1:1,000, Millipore). Next day, after rinsed with PBS, they were incubated for 2 h at room temperature with their corresponding secondary antibodies conjugated with Alexa-488 (Thermo Fisher Scientific). The primary and secondary antibodies were diluted in PBS containing 1% normal goat serum and 0.2% Triton X-100. After reaction, the sections were mounted on glass slides and cover glasses slipped in mounting medium. Fluorescent images were captured with a confocal microscope. Brain sections of each rat were chosen for staining every 6 slices, and the data are represented as the number of cells/slice or the percentage.

Statistical analysis

All data are presented as the arithmetic mean with the standard error of the mean (SEM). Data between groups were compared using Student's *t*-test or the Chi-square test. The ordinal clustering method was used for grading multiple variables. Principal component analysis (PCA) was used to assess the severity, and SPSS software was used to obtain the PC1 and PC2 scores. Finally, the k-Mean's clustering approach was used to cluster the data as 'normal condition' or 'abnormal condition'. The CDI index was defined as the ratio of the counts in the 'abnormal' cluster to the total number of data points. Data were considered significant when $P<0.05$.

Results

Biological parameters of central diabetes insipidus

Twenty rats underwent PEL, 16 survived and were included in the PEL group, and 8 underwent sham operations and exhibited long-term survival. The biological parameters of each rat were collected each day. The average daily water consumption (DWC), daily urine

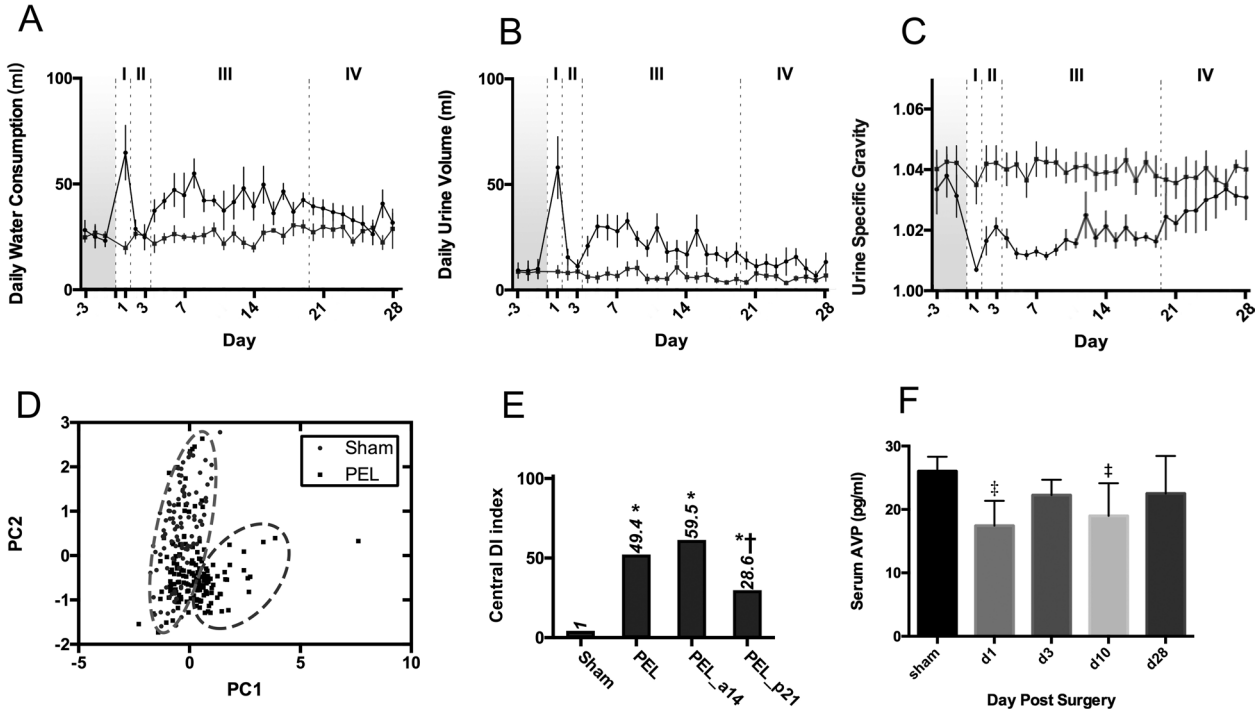

Fig. 2. Rats that underwent pituitary stalk electric lesion (PEL) exhibited a triphasic pattern of central diabetes insipidus (CDI). A–C: A time course of daily water consumption (DWC), daily urine volume (DUV), urine specific gravity (USG) after PEL. Sham-operated rats=8 (red line), PEL rats=16 (black line). DWC, DUV and USG remained relatively constant over the entire period of observation in sham rats, while there was a triphasic pattern in PEL rats. Phase I: Sharp changes during the first days after surgery; Phase II: A comparable low level with those in the control group at 2–3 d; Phase III: An increase in DWC and DUV and a decrease in USG again at 4–19 d. Phase IV: The DWC and DUV and USG recovered to baseline after 21 d. D: The 3 variables were divided into the fine cluster (blue circle) and the worse cluster (green circle). The red dots and black dots represent Sham and PEL, respectively. A portion of rats that underwent PEL were classified into the fine cluster, which was regarded as phase II or IV. E: The central diabetes insipidus index (central DI index) was compared in the Sham and PEL groups. The central DI index in the first 14 days (PEL_a14) after the operation was regarded as the severity, while the last 7 days (PEL_p21) were regarded as the recovery. F: The serum AVP levels in sham-operated rats (n=6) and in each CDI phase of PEL rats (n=6). **P*<0.01, for the difference between (PEL, PEL_a14d, PEL_p21d) vs. sham group, Chi-square, †*P*<0.05, for the difference between PEL and PEL_p21, Chi-square. ‡*P*<0.05, for the difference between sham-operated and PEL rats, One-way ANOVA.

volume (DUV) and specific gravity of urine (USG) of the sham surgery group were 24.7 ± 1.8 ml/24 h, 8.5 ± 1.8 ml/24 h and 1.037 ± 0.003, respectively, and remained relatively constant throughout the entire period of observation. PEL rats exhibited a typical tri-phasic pattern similar to DWC, DUV and USG, which can be further demarcated into 4 phases with the ordinal clustering method. Phase I (first day after surgery) displayed a sharp increase in DWC (64.7 ± 12.9 ml/24 h) and DUV (58.0 ± 14.6 ml/24 h) and a decrease in USG (1.007 ± 0.001) followed by phase II (day 2–3 post-surgery), during which the levels of DWC (26.7 ± 3.5 ml/24 h) and DUV (13.4 ± 2.3 ml/24 h) decreased and USG increased (1.019 ± 0.003). During phase III (days 4–19 post-surgery), DWC and DUV increased again to 42.8 ± 1.6 ml/24 h and 22.7 ± 1.3 ml/24 h, respectively, and remained steadily elevated, reaching a peak value on day 8, and USG stayed at a relatively lower level during this phase (1.016 ± 0.001) (Figs. 2A and B). After 20 days, these parameters returned to baseline levels, which was classified as phase IV, and shared the same cluster as the control group. In this phase, the DWC, DUV and USG of PEL were 34.3 ± 1.7 ml/24 h, 12.2 ± 1.3 ml/24 h and 1.028 ± 0.002, respectively (Figs. 2A–C). To assess the severity and recovery of CDI, all of the biological parameters were processed by PCA, and the k-mean's method was used to classify these parameters into fine or worse clusters of CDI. Most data points from the control group were assigned into the fine cluster (red dots in blue circle, Fig. 1D), and the fraction of rats that underwent PEL in phase II or IV post-surgery were classified into the fine cluster. For more than half of the

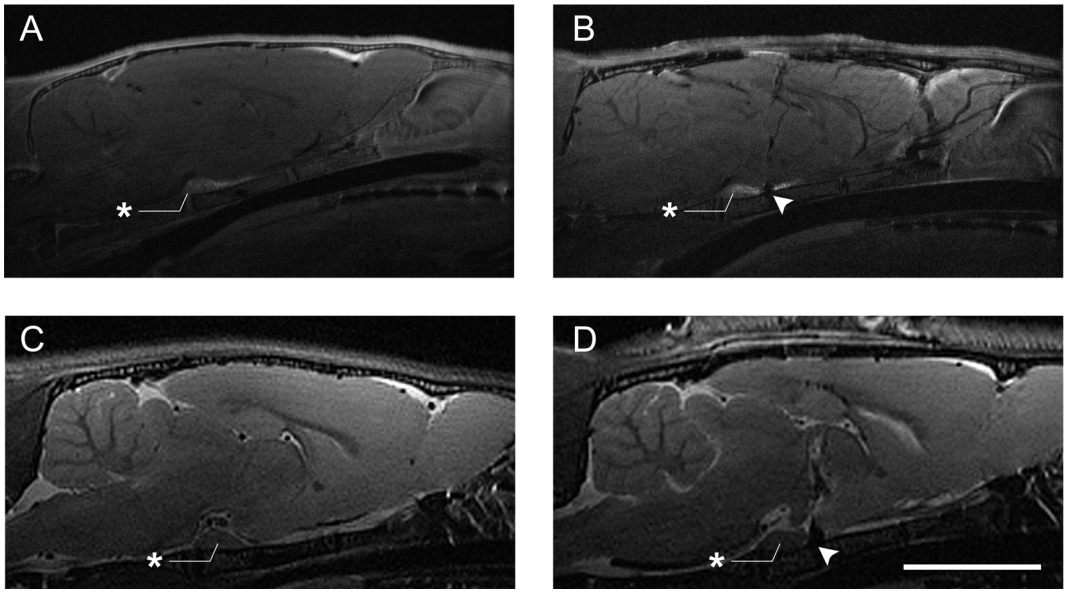

Fig. 3. MR images of control and PEL rats *in vivo*. T1-weighted images of the middle sagittal plane in control rats (A) and PEL rats 28 d after the operation (B). After Gd-DTPA administration, the signal in the hypothalamic-neurohypophysis axis was interrupted in PEL rats (arrow head). T2-weighted images of the middle sagittal plane in control rats (C) and PEL rats 28 d after the operation (D). *Represents the pituitary gland. The arrowhead indicates the lesion site. Scale bar=10 mm.

duration of the experimental period, PEL rats exhibited a fine biological characteristic and a CDI index of 49.4 (Fig. 1E). The CDI indices for the first 14 post-operative days (PEL_a14) and the last 7 days after the operation (PEL_p21) were 59.5 and 28.6, which are considered as severe and recovered, respectively. The difference between the control and PEL groups was statistically significant ($P<0.001$). Most PEL rats began to recover, as was also evident by comparing the CDIs of the PEL period and the last 7 days post-surgery (49.4 vs. 28.6, $P=0.016$). Moreover, the serum AVP concentrations in the sham-operated group was 26.0 ± 2.2 pg/ml, and the serum AVP level in each phase after PEL surgery (day 1, day 3, day 10 and day 28 after surgery) were 17.4 ± 3.9 pg/ml, 22.3 ± 2.4 pg/ml, 18.9 ± 5.1 pg/ml, 21.8 ± 5.2 pg/ml, respectively. The difference in serum AVP levels between the sham and day 1 and day 10 was statistically significant (Fig. 2F).

In vivo magnetic resonance imaging of lesion sites

Representative high-resolution MRI images are shown in Fig. 3. In the control group, hyper-intensity was particularly prominent on the T1-weighted images at the ME, pituitary stalk and the pituitary after Gd-DTPA administration. Moreover, the signals of the hypothalamic-neurohypophysis axis were continuous (Fig. 3A). Several cisterns and ventricles were clearly observed on T2-weighted images, such as the chiasmatic cistern, suprasellar cistern and the interpeduncular cistern that surrounded the pituitary. A hypo-intense signal between the cistern and the gland was identified as the diaphragma sellae (Fig. 3C). MRI scans performed in PEL rats 4 weeks after the operation showed that the lesions located in the supra-sellar region between the pituitary stalk and the pituitary gland represented by an interruption of signals of the hypothalamic-neurohypophysis axis. Increased signal intensity was observed on T1-weighted images at the proximal end after Gd-DTPA administration (Fig. 3B). On T2-weighted images, no obvious changes in the cisterns or ventricles were seen between the groups. Furthermore, no brain tissue injury, brain hematoma, cerebral infarction and hydrocephalus was detected in PEL rats (Fig. 3D).

Immunostaining for AVP

AVP immunostaining was continuous from the ME to the posterior lobe of the pituitary (PPit) in sham rats, while it was interrupted at the lesion sites in PEL rats. The pituitary of the PEL rats exhibited little or no AVP immunoreactivity (-ir) in the degenerated neural lobe 28

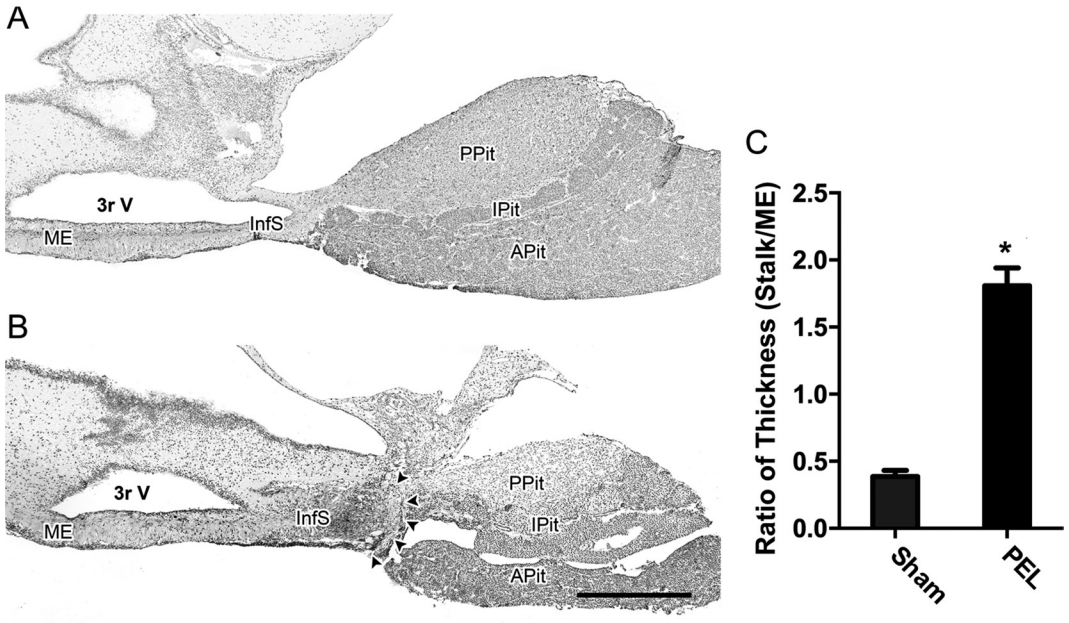

Fig. 4. The middle sagittal plane section from the sham-operated group (n=4) (A) and the PEL group (n=6) (B) stained for AVP-ir. Note the absence of AVP staining 28 days after the PEL procedure. Meanwhile, the proximal end of the pituitary stalk lesion was significantly enlarged compared to that seen in the sham rats (arrow head). This finding was accompanied by abundant AVP staining. The stalk and ME ratio provide a measure of regeneration of the pituitary stalk. The ratio in the sham and PEL was 0.39 ± 0.04 and 1.81 ± 0.13, respectively. 3rV, 3rd ventricle; APit, anterior lobe of pituitary; InfS, infundibular stem; IPit, intermediate lobe of pituitary; ME, median eminence; PPit, posterior lobe of pituitary *P<0.001 compared with sham operated rats. Scale bar=500 μm.

days after the operation. There was no evidence of extra tissue injury to either the anterior lobe of the pituitary (APit) or the intermediate lobe of the pituitary (IPit) (Figs. 4A and B). The proximal end of the site of pituitary stalk injury, which forms the ectopic neural lobe, was significantly enlarged and was also characterized by abundant AVP staining compared to the sham rats. Stalk and ME ratio which provides a measure of regeneration of pituitary stalk was 0.39 ± 0.04 and 1.81 ± 0.13 in the sham and PEL rats, respectively. (P<0.001) (Fig. 4C).

Furthermore, immunofluorescent staining for AVP was performed in the hypothalamic region using the anti-AVP antibody, and AVP-positive cells were counted in the SON and PVN. The number of AVP-positive magnocellular neurons was reduced in both the SON and PVN 28 days post-PEL compared to the sham-operated rats (Figs. 5A and B). The number of AVP-positive cells in the unilateral SON in sham and PEL rats were 132.4 ± 9.7 and 26.2 ± 3.2, respectively (P<0.001). The number of AVP-positive cells in the PVN was 137.0 ± 13.1 and 16.7 ± 2.8 in sham and PEL rats, respectively (P<0.001) (Fig. 5C).

Discussion

We designed a 3D-printed metal knife that was compatible with the stereotaxic instrument to create a standard and reproducible PEL long-term model, which induced a tri-phasic CDI in rats. In addition, we also classified the post-PEL CDI during the 4-week experimental period into four phases based on certain biological parameters. Based on these data, we have proposed a CDI index to evaluate the severity and the subsequent recovery. Finally, we performed *in vivo* MRI scans to identify the lesion sites and AVP immunostaining to track axon regeneration and the atrophy of the magnocellular nucleus, with results that were consistent with previous studies.

Neuro-lobectomy is one of the best methods to study neurohypophyseal function since the surgical removal of the neural (and intermediate) lobe can be accomplished with minimal damage to either the anterior lobe or even the rest of the brain. CDI induced by the transection of the pituitary stalk in rats was first introduced by Makara [19, 20] and Dohanics [8]. Makara constructed

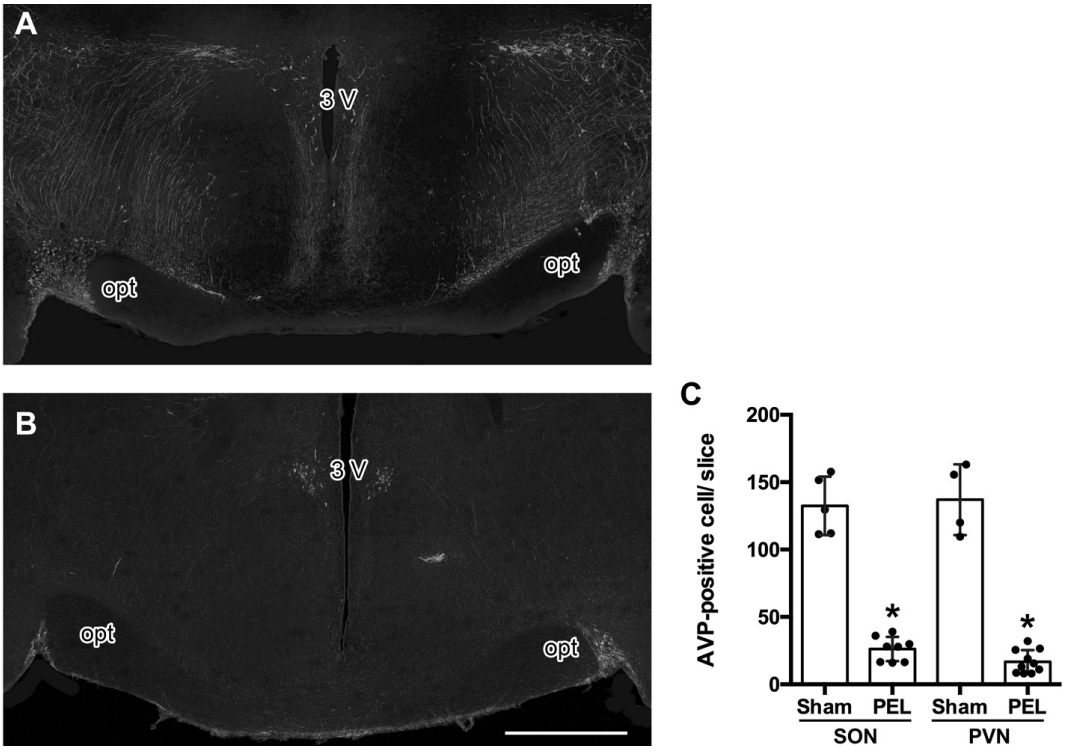

Fig. 5. A coronal plane section through the SON and PVN from sham-operated (A) and PEL rats. (B) A stain for AVP and (C) AVP-positive neurons were counted in the SON and PVN in the Sham-operated group (n=4) and the PEL group (n=10). 3rV, 3rd ventricle; opt, optic tract. *P<0.001 compared with sham-operated rats. Scale bar=1,000 μm.

four specially shaped knives and used elaborate skills to turn the angle for the denervation of the posterior pituitary (the neural lobe and the intermediate lobe) in a dorsal approach. Another lesion tool made by Dohanics was a triangular-shaped wire that could be fastened to the electrode carrier of the stereotaxic apparatus, by which the pituitary stalk was compressed directly to generate an animal model for CDI. In addition, other researchers have used the advanced method to create the CDI model [11, 17, 18]. However, the caveats included the simplicity and reproducibility of lesion tools to obtain a stable model. Therefore, we designed a lesion knife in a 3D format and printed it using a metallic material. The curved head of the knife was designed to fit with the sella of the rat skull base (120–300 g). The width was a little shorter than the distance between the medial walls of the bilateral V nerve. The optimal thickness of the knife was achieved with the help of the latest 3-D printer specifications. This tool was therefore equipped to apply both the electric lesions as well as the compression during the surgical procedure.

The pattern of biological parameters in rats with CDI differs depending on the triggering method used [5, 6, 8, 11, 25]. In this study, we used DWC, DUV and daily USG as the evaluation parameters since they are easy to observe and record. The course of postoperative CDI can be transient, permanent or tri-phasic in patients with pituitary damage. The tri-phasic pattern occurs in 3.4% of patients who undergo trans-sphenoid surgery, and only the first 2 phases occur in 1.1% of those patients with pituitary damage [14]. In this study, we classified four distinct CDI stages during a four-week post-operative period with the help of the ordinal clustering method. In phase I, i.e., the day after the surgery, DWC and DUV increased dramatically while USG was significantly lower than 1.010. Phase II was seen between 2–3 days post-surgery with low levels of DWC and DUV and high USG. Phase III, ranging from days 4–19 post surgery, was also characterized by polydipsia and polyuria, which peaked on day 8. Finally, the biological parameters returned to normal after 20 days, and the animals entered Phase IV.

We have posed a hypothesis to explain the mechanism behind this multi-phasic CDI. The polydipsia and poly-

uria seen in phase I could be a result of a temporary dysfunction of AVP-secreting neurons, either due to disrupted connections between the body of the magnocellular neurons and the nerve terminals in the posterior pituitary or due to the destruction of the vascular supply in the nerve perturbations. This finding is likely followed by an uncontrolled release of AVP or OXT from either the degenerating posterior pituitary tissue or from the remaining magnocellular neurons, resulting in the changes seen in phase II [10]. Other possible reasons for phase II could be an up-regulation of dendritic secretion or increased neurohypophyseal hormone secretion into the peripheral circulation through the cerebrospinal fluid [15]. The third phase of CDI follows the depletion of AVP that results from the degeneration of hypothalamic AVP and OXT-secreting neuronal cell bodies. With the passage of time, magnocellular cells in the SON and PVN were gradually lost due to apoptosis, leading to insufficient AVP and OXT to maintain the normal level of urination and balance of electrolytes and fluids, a feature that is permanent in some patients [10]. However, in our study, the animals exhibited a recovery phase, or phase IV, which is likely due to neuronal and axonal regeneration in the ectopic neural lobe and to angiogenesis [26–30].

Although the time course for the biological parameters of CDI during the post-operative period was easy to depict, it was still difficult to measure the CDI severity and recovery in rats. We have therefore proposed a CDI index, which is defined as the ratio of the number of data points in the abnormal cluster to the total data points. Based on the four-phase division of CDI as described above, we defined the CDI index during the first 14 days post-surgery as severe (a14d), when a longer duration i.e., more days of CDI symptoms corresponded to a worse situation and a higher grade of CDI index. Similarly, the CDI index of the last 7 days (p21d) was represented as the recovery phase in this study. The advantage of this CDI index assessment system was that multiple parameters could be incorporated.

In addition to the measurement of biological parameters, we also performed imaging studies to locate the precise sites of the lesions and confirm the accuracy of the surgical operation without sacrificing the animals and staining brain sections. MRI could capture enhanced T1-weighted and T2-weighted sagittal images in the control rats. The pituitary stalk lies over the sella and is linked to the pituitary to form a PPit, which emitted high signal in contrast enhanced T1-weighted images. The reason for such high signals was that the MRI reagents could easily penetrate the tissues on account of a lack of any blood-brain barrier (BBB) as well as the unmyelinated nature of the magnocellular nerve projections in the pituitary stalk [24]. The PEL procedure completely disrupted the continuous high signal of pituitary stalk, indicating surgical success.

The number of AVP-positive cells can be regarded as an alternative assessment of injury since the mid-sagittal plane displays the lesion site clearly following AVP or OXT staining [8]. In our study, few AVP-ir cells were seen in the PPit after PEL surgery. In addition, not only was the number of magnocellular cells decreased, but the length and number of dendrites of those cells also degenerated over time.

With serum AVP detected and biological characteristics analysis, we found that rats with PEL can recover from CDI after a long time, despite there is few AVP-ir cells in the SON and PVN we observed, we assume that, there are still some gliocytes in SON and PVN which might enhance the ability of the remained AVP neurons as compensation after PEL. Secondly, in the later pattern after PEL, AVP synthesized by the remaining functional AVP neurons in the SON, PVN may be released into the circulation directly rather than transported to the neural pituitary for an interruption of the pituitary stalk to maintain the AVP levels in circulation. More importantly, as shown in Fig. 3, there is an enlarged end proximal to the injury site with strongly positive AVP immunostaining. An enlarged pituitary stalk may play roles in helping PEL rats recover from CDI in the 4th phase. These findings may require further studies to confirm the data.

Also, there are also some limitations in this study. First, PEL operation was successfully performed in adult rats, but further investigation is required to determine whether it is suitable for other mammals. Second, the PEL surgery approach is not the same as the clinical surgery approach to deal with sellar disease, which may cause different complications that we cannot detect in this study. Last but not the least, although we targeted at pituitary stalk as precisely as possible by using stereotactic equipment, we could not identify the functional cell type which mediates the CDI condition, as all types of cells at injury sites are affected. To meet these need, cre-loxp gene-editing system, transgenetic method, optogenetics and chemical genetics can be used to investigate the mechanism behind CDI in future research.

The hypothalamus is an important control center for normal physiological functions, and even a slight disturbance may lead to fatal complications. Nevertheless, the survival rate is very high in rats that receive hypothalamic surgery, making them a suitable model for neurological studies. In our study, we assumed that intracranial hematomas in the sellae were the main causes of short-term deaths. In rats that survived for a longer period of time, anhormonia, unconsciousness, and adipsia, a severe situation seen after sellar surgery [7, 16], may result in the loss of initiative to drink water. This feature further induced homeostatic dysfunction, a drastic drop in urine output and an accompanying consciousness disorder, which resulted in a worse prognosis for survival.

In conclusion, we established a stable and reproducible PEL model using a 3D-printed knife and classified the CDI period into 4 phases after surgery with three biological parameters. In addition, we also proposed a CDI index to assess the severity and recovery of CDI in rats. Additionally, MRI and immunostaining of brain slices were used to identify the lesion sites. Our study indicated that complete interruption of the MRI signal, reduction in magnocellular neuron counts and absence of AVP expression in the posterior lobe of the pituitary gland could be used as the "gold standard" for successful PEL.

Acknowledgments

This work was supported by the National Key Technology Research and Development Program of the Ministry of Science and Technology of China grant 2014BAI04B01, Science and Technology Planning Project of Guangdong Province, China grant 2016A020213006 and 2017A030303021.

References

1. Adams, J.H., Daniel, P.M., and Prichard, M.M. 1968. The vascular anatomy of the ferret's pituitary and its relevance to the consequences of stalk section. *J. Physiol.* 196: 101P–102P. [Medline]
2. Adams, J.H., Daniel, P.M., and Prichard, M.M. 1969. Degeneration and regeneration of hypothalamic nerve fibers in the neurohypophysis after pituitary stalk section in the ferret. *J. Comp. Neurol.* 135: 121–144. [Medline] [CrossRef]
3. Adams, J.H., Daniel, P.M., and Prichard, M.M. 1963. Volume of the infarct in the anterior lobe of the monkey's pituitary gland shortly after stalk section. *Nature* 198: 1205–1206. [Medline] [CrossRef]
4. Adams, J.H., Daniel, P.M., and Prichard, M.M. 1963. The volumes of pars distalis, pars intermedia and infundibular process of the pituitary gland of the rat, with special reference to the effect of stalk section. *Q. J. Exp. Physiol. Cogn. Med. Sci.* 48: 217–234. [Medline]
5. Bernal, A., Mahía, J., and Puerto, A. 2013. Differential lasting inhibitory effects of oxytocin and food-deprivation on mediobasal hypothalamic polydipsia. *Brain Res. Bull.* 94: 40–48. [Medline] [CrossRef]
6. Bernal, A., Mahía, J., and Puerto, A. 2016. Animal models of Central Diabetes Insipidus: Human relevance of acquired beyond hereditary syndromes and the role of oxytocin. *Neurosci. Biobehav. Rev.* 66: 1–14. [Medline] [CrossRef]
7. Di Iorgi, N., Morana, G., Napoli, F., Allegri, A.E., Rossi, A., and Maghnie, M. 2015. Management of diabetes insipidus and adipsia in the child. *Best Pract. Res. Clin. Endocrinol. Metab.* 29: 415–436. [Medline] [CrossRef]
8. Dohanics, J., Hoffman, G.E., Smith, M.S., and Verbalis, J.G. 1992. Functional neurolobectomy induced by controlled compression of the pituitary stalk. *Brain Res.* 575: 215–222. [Medline] [CrossRef]
9. Dyball, R.E. and Koizumi, K. 1969. Electrical activity in the supraoptic and paraventricular nuclei associated with neurohypophysial hormone release. *J. Physiol.* 201: 711–722. [Medline] [CrossRef]
10. Edate, S. and Albanese, A. 2015. Management of electrolyte and fluid disorders after brain surgery for pituitary/suprasellar tumours. *Horm. Res. Paediatr.* 83: 293–301. [Medline] [CrossRef]
11. Elias, P.C., Elias, L.L., Castro, M., Antunes-Rodrigues, J., and Moreira, A.C. 2004. Hypothalamic-pituitary-adrenal axis up-regulation in rats submitted to pituitary stalk compression. *J. Endocrinol.* 180: 297–302. [Medline] [CrossRef]
12. Falconi, G. and Rossi, G.L. 1964. Transauricular hypophysectomy in rats and mice. *Endocrinology* 74: 301–303. [Medline] [CrossRef]
13. Haller, J., Makara, G.B., Barna, I., Kovács, K., Nagy, J., and Vecsernyés, M. 1996. Compression of the pituitary stalk elicits chronic increases in CSF vasopressin, oxytocin as well as in social investigation and aggressiveness. *J. Neuroendocrinol.* 8: 361–365. [Medline] [CrossRef]
14. Hensen, J., Henig, A., Fahlbusch, R., Meyer, M., Boehnert, M., and Buchfelder, M. 1999. Prevalence, predictors and patterns of postoperative polyuria and hyponatraemia in the immediate course after transsphenoidal surgery for pituitary adenomas. *Clin. Endocrinol. (Oxf.)* 50: 431–439. [Medline] [CrossRef]
15. Higashida, H. 2016. Somato-axodendritic release of oxytocin into the brain due to calcium amplification is essential for social memory. *J. Physiol. Sci.* 66: 275–282. [Medline] [CrossRef]
16. Kinsman, B.J., Nation, H.N., and Stocker, S.D. 2017. Hypothalamic Signaling in Body Fluid Homeostasis and Hypertension. *Curr. Hypertens. Rep.* 19: 50. [Medline] [CrossRef]
17. Mahía, J., Bernal, A., and Puerto, A. 2008. NaCl preference and water intake effects of food availability in median

eminence polydipsia. *Neurosci. Lett.* 447: 7–11. [Medline] [CrossRef]
18. Mahía, J. and Puerto, A. 2006. Lesions of tuberomammillary nuclei induce differential polydipsic and hyperphagic effects. *Eur. J. Neurosci.* 23: 1321–1331. [Medline] [CrossRef]
19. Makara, G.B. 1993. Denervation of the rat posterior pituitary gland: validation of a stereotaxic method. *J. Neuroendocrinol.* 5: 335–340. [Medline] [CrossRef]
20. Makara, G.B., Sutton, S., Otto, S., and Plotsky, P.M. 1995. Marked changes of arginine vasopressin, oxytocin, and corticotropin-releasing hormone in hypophysial portal plasma after pituitary stalk damage in the rat. *Endocrinology* 136: 1864–1868. [Medline] [CrossRef]
21. Meyer-Lindenberg, A., Domes, G., Kirsch, P., and Heinrichs, M. 2011. Oxytocin and vasopressin in the human brain: social neuropeptides for translational medicine. *Nat. Rev. Neurosci.* 12: 524–538. [Medline] [CrossRef]
22. Ng, L.K., Douthitt, T.C., Thoa, N.B., and Albert, C.A. 1975. Modification of morphine-withdrawal syndrome in rats following transauricular electrostimulation: an experimental paradigm for auricular electroacupuncture. *Biol. Psychiatry* 10: 575–580. [Medline]
23. Smith, P.E. 1930. Hypophysectomy and a replacement therapy in the rat. *Am. J. Anat.* 45: 205–273. [CrossRef]
24. Theunissen, E., Baeten, K., Vanormelingen, L., Lambrichts, I., Beuls, E., Gelan, J., and Adriaensens, P. 2010. Detailed visualization of the functional regions of the rat pituitary gland by high-resolution T2-weighted MRI. *Anat. Histol. Embryol.* 39: 194–200. [Medline] [CrossRef]
25. Wang, Y., Zhao, C., Wang, Z., Wang, C., Feng, W., Huang, L., Zhang, J., and Qi, S. 2008. Apoptosis of supraoptic AVP neurons is involved in the development of central diabetes insipidus after hypophysectomy in rats. *BMC Neurosci.* 9: 54. [Medline] [CrossRef]
26. Wu, W. and Scott, D.E. 1993. Increased expression of nitric oxide synthase in hypothalamic neuronal regeneration. *Exp. Neurol.* 121: 279–283. [Medline] [CrossRef]
27. Wu, W.T., Scott, D.E., and Gilman, A.M. 1989. Correlative scanning-immunoelectromicroscopic analysis of neuropeptide localization and neuronal plasticity in the endocrine hypothalamus. *Brain Res. Bull.* 22: 399–410. [Medline] [CrossRef]
28. Yuan, Q., Scott, D.E., So, K.F., and Wu, W. 2007. A subpopulation of reactive astrocytes at affected neuronal perikarya after hypophysectomy in adult rats. *Brain Res.* 1159: 18–27. [Medline] [CrossRef]
29. Yuan, Q., Scott, D.E., So, K.F., and Wu, W. 2007. Differential activation of c-fos immunoreactivity after hypophysectomy in developing and adult rats. *Anat. Rec. (Hoboken)* 290: 1050–1056. [Medline] [CrossRef]
30. Yuan, Q., Scott, D.E., So, K.F., Lin, Z., and Wu, W. 2009. The potential role of nitric oxide synthase in survival and regeneration of magnocellular neurons of hypothalamo-neurohypophyseal system. *Neurochem. Res.* 34: 1907–1913. [Medline] [CrossRef]